Optimal Placement of UPFC for Maximizing System Loadability and Minimize Active Power Losses by NSGA-II

I Made Wartana*, *Student Member, IEEE,* Jai Govind Singh†, *Member, IEEE*, Weerakorn Ongsakul, *Member, IEEE,* Kittavit Buayai, and Sasidharan Sreedharan

Abstract**-- This paper presented application of a new variant of Genetic Algorithm, specialized in multi-objective optimizations problem known as Non-dominated Sorting Genetic Algorithm II (NSGA-II), to obtain the optimal allocation of Unified Power Flow Controller (UPFC) for enhancing the power system loadability as well as minimizing the active power loss in transmission line. An Optimal Power Flow (OPF) problem with mixed integer programming has been formulated for optimizing the above two objectives as well as obtaining the optimal location of the UPFC while maintaining the system security and stability margins, e.g., small signal stability, voltage stability index, and line stability factor. In addition, a fuzzy based mechanism has been employed to extract the best compromise solution from the Pareto front. The effectiveness of the proposed methodology has been investigated on a standard IEEE 30-bus and practical Java-Bali 24-bus of Indonesian systems. Results demonstrate that the static and dynamic performances of the power system can be effectively enhanced by the optimal allocation of the UPFC. Moreover, UPFC installation cost is also calculated and overall performance has been compared with existing method.**

Index Terms**-- Multi-objective optimization, NSGA-II, stability margin, system loadability, UPFC**

I. INTRODUCTION

IN recent decades, the actual power systems are facing new challenges due to deregulation and restructuring of the electricity market. It has become imperative to better utilize the existing power networks to increase capacities by installing FACTS controllers [1]. The variables and parameter of the transmission line, which include line reactance, voltage magnitude, and phase angle are able to be controlled using FACTS controllers in a fast and effective way [2]. The benefits derived from FACTS include improvement of the stability of power system networks, such as the small signal stability, transient stability, and thus enhance system reliability. However, controlling power flows is the main function of FACTS [3],[4]. Maximal system loadability can also be obtained with the optimal location and parameter setting of FACTS controllers [5],[6]. These basic ideas behind the FACTS concept play an active role in the operation and control of competitive power systems.

The maximum benefit of the FACTS controllers depends greatly on how these controllers are allocated in the power system: namely, on their location and settings [4]. The range of FACTS controllers includes: Static Var Compensator (SVC); Thyristor Controlled Series Compensator (TCSC); Unified Power Flow Controller (UPFC); and Static Compensator (STATCOM).

In the last few years, in the research arena of computational intelligence, several cooperative and competitive stochastic search techniques have rapidly gained popularity as efficient optimization techniques. Such techniques include a hybrid Tabu Search (TS) and Simulated Annealing (SA) [7], Evolutionary Programming (EP) [8], Genetic Algorithm (GA) [9],[10], Bacterial Swarming Algorithm (BSA) [11], and Particle Swarm Optimization (PSO) [12],[13]. The GA and PSO techniques have been formulated to solve optimal location and parameter settings of multiple TCSCs and UPFCs to increase power system loadability [13],[14]. The application of PSO technique for optimal location of multiple FACTS controllers, taking into consideration the cost of installation and the system loadability, has been reported [5], [14]. From the previous works, it can be concluded that the problem of optimal location of FACTS controllers is generally formulated as a mono-objective optimization problem. Unfortunately, the formulation of FACTS location problem as a mono-objective optimization is not quite practical. While, planners the power systems aim to take advantage of FACTS controllers considering several objectives at the same time.

In contrary to the previous cited works, Benadid et al. [15] formulates the optimal UPFC placement using hierarchical multi-objective optimization algorithms. Where, the problem is formulated as a bi-objective optimization problem. The UPFCs are optimized in order to analyze the impact of the

*I Made Wartana would like to acknowledge the financial support provided by the Directorate General of Higher Education of the Republic of Indonesia under Grant DIKTI-Scholarship 2008, and his employer, i.e., National Institute of Technology (ITN), East Java-65145, Indonesia, for providing the study leave as well as other support to pursue for his doctoral degree at the Asian Institute of Technology, Thailand.

†Corresponding author.

I Made Wartana (Email: I.Made.Wartana@ait.ac.th), Jai Govind Singh (Email: jgsingh@ait.ac.th, phone: (66-2) 524-5426; fax: (66-2) 524-5439), Weerakorn Ongsakul (Email: ongsakul@ait.asia) and Kittavit Buayai (Email: kittavit.buayai@ait.ac.th) are with the Energy field of Study, SERD, Asian Institute of Technology, Pathumthani 12120, Thailand.

Sasidharan Sreedharan (Email: sasiait@gmail.com).

UPFC on the static voltage stability and real power losses. However, the dynamic performance base on small signal stability considering the investment cost of UPFC device and their impact on placement to maximize system loadability in the network are not wholly considered yet.

In this paper, an algorithm of the optimal placement of one type of FACTS controllers, UPFC, is developed as a multi-objective problem to maximize system loadability within system security and stability margin i.e., small signal stability, voltage stability index, and line stability factor. By means of UPFC optimal placement, the active power losses of the transmission system is minimize whereas the system loadability of the transmission lines is maximized. In realizing the proposed objectives, the suitable location of UPFC and its rated values must be determined simultaneously. In doing so, the NSGA-II is used.

The paper is organized into six sections, beginning with an introduction, followed by Section 2 which presents the modeling of UPFC. The problem formulation is proposed in Section 3 which includes the definition of objective functions and problem constraints. Section 4 presents the implementation of the NSGA-II algorithm. Some interesting results are presented along with a detailed discussion in Section 5. Finally, conclusions and major contributions are summarized in Section 6.

II. Component Modeling

A. Static Model of UPFC

The UPFC has two voltage source inverters (VSI) sharing a common dc storage capacitor. It is connected to the system through two coupling transformers [16],[17] as shown in Fig. 1. The UPFC model is represented by one series voltage source v_s and by another shunt current source i_{SH}. In this study, UPFC has been assumed to be placed at bus-*i* and in line connected between bus-*i* and bus-*j*. The series voltage source and the shunt current source of UPFC are defined as follows:

$$\left.\begin{aligned} \overline{v_S} &= (v_p + v_q)e^{j\varphi} = r\overline{V_i}e^{j\gamma} \\ \overline{i_{SH}} &= (i_p + i_q)e^{j\theta_i} \end{aligned}\right\} \quad (1)$$

The equations of the apparent power injected by the UPFC at bus-*i* and bus-*j*, while placed at bus-*i*, are $P_{iju}+jQ_{iju}$ and $P_{jiu}+jQ_{jiu}$, respectively, and given as follow.

$$\left.\begin{aligned} P_{iju} &= brV_iV_j\sin(\gamma + \theta_i - \theta_j) \\ Q_{iju} &= brV_i^2\cos\gamma - i_qV_i \\ P_{jiu} &= -brV_iV_j\sin(\gamma + \theta_i - \theta_j) \\ Q_{jiu} &= -brV_iV_j\cos(\gamma + \theta_i - \theta_j) \end{aligned}\right\} \quad (2)$$

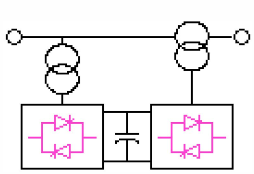

Fig. 1. Model of UPFC

where, v_p and v_q are the component of v_s that are in phase and in quadrant, respectively, with the line current. i_q represents the component of shunt current i_{SH} that is in phase with the bus voltage V_i which keeps the bus voltage around a specified level through the regulator gain K_r. θ_i and θ_j are the voltage angle of sending and receiving ends, respectively, of UPFC bus. r is the relative magnitude and γ is the relative phase angle, both are with respect to V_i, where $b = 1 / X_s$, with X_s as line reactance.

B. Dynamic Model of UPFC

The UPFC dynamic model [16] has a 3rd order. Observe that the Power System Oscillator Damper (POD) controller could be used to modulate whatever of UPFC variables (v_p, v_q, i_q). The set of differential equations are as follows:

$$\left.\begin{aligned} \dot{v}_p &= \frac{1}{T_r}\left(v_{p0} + u_1 v_{POD} - v_p\right) \\ \dot{v}_q &= \frac{1}{T_r}\left(v_{q0} + u_2 v_{POD} - v_q\right) \\ \dot{i}_q &= \frac{1}{T_r}\left[K_r\left(V_{ref} + u_3 v_{POD} - V_k\right) - i_q\right] \end{aligned}\right\} \quad (3)$$

Where, u_1, u_2 and u_3 are 1 if the corresponding stabilizing POD signal is enabled, 0 otherwise. K_r and T_r are regulator gain and time constant, respectively, of the UPFC regulator. V_{ref} is the voltage reference of the UPFC regulator. In steady-state, the input v_{p0} and v_{q0} are set to zero.

III. Problem Formulation

As indicated, the goal of optimization is the optimal placement of UPFC into power network in order to maximize the system loadability within security and stability margins and minimize the real power loss in transmission lines. The optimization problem is formulated as bi-objective optimization problems; maximizing the power system loadability within security and stability margins and minimizing the real power loss objectives by considering the investment costs of UPFC device.

Therefore, the presented problem becomes a multi-objective optimization problem that has two objective functions to be optimized simultaneously, which can be denoted as:

$$\text{Minimize } F(\mathbf{x},\mathbf{u}) = [F_1(\mathbf{x},\mathbf{u}),\ F_2(\mathbf{x},\mathbf{u})] \quad (4)$$

$$\text{Subject to}: \begin{cases} g(\mathbf{x},\mathbf{u}) = 0 & j = 1,\ldots, M \\ h(\mathbf{x},\mathbf{u}) \le 0 & k = 1,\ldots, K \end{cases} \quad (5)$$

Where, F is known as the objective vector, F_1 and F_2 are the two objective functions to be optimized, $\mathbf{x}$ is the vector of dependent variables, and $\mathbf{u}$ is the vector of control variables.

The optimal location and settings of UPFC is formulated as a real constrained mixed discrete continuous multi-objective optimization problem.

The objective functions considered in this paper are presented in detail below.

A. Maximize the System Loadability within Security Margins

$$\text{Maximize } F_2(\mathbf{x},\mathbf{u}) = \{\lambda_1\} \quad (6)$$

$$\text{Subject to } VL = \sum_{i=1}^{N_l} OLL_i \times \sum_{j=1}^{N_b} BVV_j \quad (7)$$

where, VL [11] is the thermal and bus violation limit factor, OLL_i and BVV_j represent the overloaded line factor and branch the bus voltage violation factor, respectively; and is elaborated in (11) and (12); N_l and N_b are the total numbers of transmission lines and load buses, respectively. In addition λ_1 is a load parameter of the system, which intends to locate the maximum sum of power that the network is able to supply within the system security margin.

The load parameter λ_1 in (6) is defined as a function of a load factor λ_f:

$$\lambda_1 = \exp[\eta|\lambda_f - \lambda_f^{\max}|] \qquad \lambda_f \in [1, \lambda_f^{\max}] \quad (8)$$

Where, η is the coefficient to adjust the slope of the function, and λ_f^{max} is the maximal limit of λ_f. The load factor λ_f reflects the variation of power loads P_{Li} and Q_{Li}, which are defined as [11],[18]:

$$P_{Li}(\lambda_f) = \lambda_f P_{Li} \qquad ; \text{i}=m+1\ldots\ldots, N_b \quad (9)$$

$$Q_{Li}(\lambda_f) = \lambda_f Q_{Li} \qquad ; \text{i}=m+1\ldots\ldots, N_b \quad (10)$$

Where, m is the total number of generator buses, $\lambda_f = 1$ indicates the base load case.

The indexes of the system security state consist of two parts. The first part, OLL_i, relates to the branch loading and penalizes overloads in the lines. The value of OLL_i equals to 1 if the jth branch loading is less than its rating. OLL_i increases logarithmly (actual logarithm) with the overload and it can be calculated from:

$$OLL_i = \begin{cases} 1; & \text{if} \quad P_{ij} \le P_{ij}^{\max}, \\ \exp\left(\Gamma_{OLL}\left|1 - \frac{P_{ij}}{P_{ij}^{\max}}\right|\right); & \text{if} \quad P_{ij} > P_{ij}^{\max}, \end{cases} \quad (11)$$

Where, P_{ij} and P_{ij}^{max} are the real power flow between buses-i and j and the thermal limit for the line between buses-i and j, respectively. Γ_{OLL} is the coefficient which is used to adjust the slope of the exponential function.

The second part BVV_j in (12) concerns the voltage levels for each bus of the power network. The value of BVV_j is defined as:

$$BVV_j = \begin{cases} 1; & \text{if } 0.9 \le V_b \le 1.1 \\ \exp(\Gamma_{BVV}|1 - V_b|); & \text{otherwise} \end{cases} \quad (12)$$

Where, BVV_j is the bus voltage violation factor at bus-j and Γ_{BVV} represents the coefficient used to adjust the slope of the exponential function in the above equation. Equation (12) shows that appropriate voltage magnitudes are close to 1 p.u. Similar to OLL_i, the value of BVV_j is equal to 1 if the voltage level falls between the minimal and maximal voltage limits. Outside the range, BVV_j increases exponentially with the voltage variation.

B. Minimization of Active Power Loss of the Transmission Lines

This objective is to minimize the active power losses (P_{loss}) in the transmission lines and which can be expressed as [15]:

$$F_2(\mathbf{x},\mathbf{u}) = \sum_{k=1}^{N_l} g_k \left[V_i^2 + V_i^2 - 2V_iV_j \cos t(\delta_i - \delta_j\right] \quad (13)$$

Where, N_l is the number of transmission lines; g_k is the conductance of the k^{th} line; $V_i\angle\delta_i$ and $V_j\angle\delta_j$ are the voltages at the end buses-i and j of the k^{th} line, respectively.

C. The UPFC Cost Function.

The installation cost (IC) of UPFC has been mathematically formulated and is given by [5],[13].

$$F_3(\mathbf{x},\mathbf{u}) = C_{UPFC}(f) \times S \times 1000 \quad (14)$$

Where $F_3(\mathbf{x},\mathbf{u})$ is the optimal installation cost of UPFC in US$, C_{UPFC} *(f)* is the installation cost of UPFC in US$/kVAR and f is vector that represents the variable of UPFC. Based on the Siemens AG Database [5],[10] the cost functions for FACTS controllers are developed. The cost for UPFC:

$$C_{UPFC} = 0.0003S^2 - 0.2691S + 188.22 \quad (15)$$

Where, C_{UPFC} is in US$/kVAR and S is the operating range of the UPFC in MVAR.

$$S = |Q_2| - |Q_1| \quad (16)$$

Where, Q_2 is the reactive power flow in the line after installing UPFC in MVAR and Q_1 is the reactive power flow in the line before installing UPFC in MVAR.

D. Dependent and Control Variables

In the two objective functions, $\mathbf{x}$ is the vector of dependent variables such as slack bus power P_{G1}, load bus voltage $V_{m+1\ldots\ldots Nb}$, generator reactive power outputs Q_G and apparent power flow S_k; $\mathbf{x}$ can be expressed as:

$$\mathbf{x}^T = [P_{G_1}, V_{m+1} \ldots V_{N_b}, Q_{G_1} \ldots Q_{G_m}, S_1 \ldots S_{N_l}] \quad (17)$$

Furthermore, $\mathbf{u}$ is a set of the control variables, such as generator real power outputs P_G except at the slack bus P_{G1}, generator voltages V_G, and the locations of UPFC device, L, and their parameter settings. $\mathbf{u}$ can be expressed as:

$$\mathbf{u}^T = [P_{G_2} \ldots P_{G_m}, V_{G_2} \ldots V_{G_m}, L, v_S, i_{SH}, \lambda_f] \quad (18)$$

The equality and inequality constraints of the Newton Raphson Power Flow (NRPF) problem incorporating UPFC are given in following subsection.

E. Equality Constraints

These constraints represent the typical load flow equations as follows:

$$P_{G_i} = P_{L_i} + V_i \sum_{i=1}^{N_b} V_j \left(G_{ij} \cos\delta_{ij} + B_{ij} \sin\delta_{ij}\right); \; 1 = 1,2,3 \ldots N_b \quad (19)$$

$$Q_{G_i} = Q_{L_i} + V_i \sum_{i=1}^{N_b} V_j \left(G_{ij} \sin\delta_{ij} - B_{ij} \cos\delta_{ij}\right); \; 1 = 1,2,3 \ldots N_b \quad (20)$$

Where, N_b is the number of buses in the system.

F. Inequality Constraints

The inequality constraints *h(***x, u***)* are limits of control variables and state variables. Generator active power P_G, reactive power Q_G, voltage V_i, and phase angle δ_i are restricted by their limits as follows:

$$\left.\begin{array}{ll} P_{G_i}^{\min} \le P_{G_i} \le P_{G_i}^{\max} & i = 1,......,m \\ Q_{G_i}^{\min} \le Q_{G_i} \le Q_{G_i}^{\max} & i = 1,......,m \\ V_i^{\min} \le V_i \le V_i^{\max} & i = 1,.......,N_b \\ -0.9 \le \delta_i \le 0.9 & i = 1,.......,N_b \end{array}\right\} \quad (21)$$

The parameter settings of UPFC are restricted by their limits as follows:

$$\left.\begin{array}{l} v_S^{\min} \le v_S \le v_S^{\max} \\ i_{SH}^{\min} \le i_{SH} \le i_{SH}^{\max} \end{array}\right\} \quad (22)$$

The constraint of transmission loading P_{ij} is represented as

$$\left|P_{ij}\right| \le P_{ij}^{\max}; \quad ij = 1,.......,N_l \quad (23)$$

The load factor λ_f is constrained by its limits as:

$$1 \le \lambda_f \le \lambda_f^{\max} \quad (24)$$

G. Power System Stability Constraints

a) Small Signal Stability

The system used for the small signal stability analysis is a differential algebraic equation (DAE) set, in the form:

$$\left.\begin{array}{l} \dot{x} = f(\mathbf{x},\mathbf{y}) \\ 0 = g(\mathbf{x},\mathbf{y}) \end{array}\right\} \quad (25)$$

Where, **x** is the vector of the state variables and **y** the vector of the algebraic variables, which are only voltages amplitudes V and phases θ. The system state matrix A_s is thus computed by manipulating the complete Jacobian matrix A_c, which is defined by the linearization of the DAE system equations (26) as follow.

$$\begin{bmatrix} \Delta\dot{\mathbf{x}} \\ 0 \end{bmatrix} = \begin{bmatrix} \nabla_x f & \nabla_y f \\ \nabla_x g & \nabla_y g \end{bmatrix} \begin{bmatrix} \Delta\mathbf{x} \\ \Delta\mathbf{y} \end{bmatrix} = \begin{bmatrix} F_x & F_y \\ G_x & G_y \end{bmatrix} \begin{bmatrix} \Delta\mathbf{x} \\ \Delta\mathbf{y} \end{bmatrix} = \begin{bmatrix} A_c \end{bmatrix} \begin{bmatrix} \Delta\mathbf{x} \\ \Delta\mathbf{y} \end{bmatrix} \quad (26)$$

The state matrix A_s is simply obtained by eliminating the algebraic variables as follow.

$$A_s = F_x - F_y G_y^{-1} G_x \quad (27)$$

Where, F_x, F_y, G_x, G_y are Jacobian Matrices as given in (26).

If the complex eigenvalues of the linearized system have negative real parts, then the power system would be able to withstand small disturbances and is thus, considered stable in the small-signal sense. The eigenvalue stability analysis is incorporated in the constraint by the equation in PSAT [16]:

$$E_i(F_x, F_y, G_y, G_x) = 0 \quad (28)$$

The eigenvalue based stability assures grid stability under various levels of system loadability.

b) Fast Voltage Stability Index

Fast Voltage Stability Index (*FVSI*) proposed by Musirin [19] is utilized in this paper to assure the safe bus loading.

$$FVSI_{ij} = \frac{4Z^2 Q_j}{V_i^2 X} \quad (29)$$

The line that exhibits *FVSI* close to 1.00 implies that it is approaching its instability point. If *FVSI* goes beyond 1.00, one of the buses connected to the line will experience a sudden voltage drop leading to the collapse of the system. *FVSI* index incorporation in the controller assures that no bus will collapse due to overloading.

c) Line Stability Factor

System Stability Index is also assured by Line Stability Factor (*LQP*) proposed by A Mohamed et al [20]. The *LQP* should be less than 1.00 to maintain a stable system.

$$LQP = 4\left(\frac{X}{V_i^2}\right)\left(\frac{X}{V_i^2} P_i^2 + Q_j\right) \quad (30)$$

LQP assure the controller that no line is over loaded under any grid condition.

IV. Non-Dominated Sorting Genetic Algorithm

A. NSGA-II

The capabilities of multi-objective genetic algorithms (MOGAs) to explore and discover Pareto optimal fronts on multi-objective optimization problems have been well recognized. It has been shown that MOGAs outperform traditional deterministic methods to this type of problem due to their capacity to explore and combine various solutions to find the Pareto front in a single run. We will implement a multi-objective optimization technique called the Non-Dominated Sorting Genetic Algorithm II (NSGA-II), which is described in detail by Deb et al. [21]. Fig. 2 shows the procedure of a one iteration of NSGA II. The NSGA-II algorithm may be stated as follows [22]:

For each iteration *k* do:

1) $R^k = P^k \cup Q^k$ (combine parent and offspring population)
2) F=non_random_sort (R^k) (Application the non-dominated sorting on (R^k))
3) $P^{k+1} = \Phi$ and i=1
4) Until $|P^{k+1}|+|F_i| \le N$ (until the parent population is filled)
   a. i=i+1
   b. Calculate the crowding distance for each particle in F_i
   c. $P^{k+i} = P^{k+1} \cup F_i$
5) Sort (F_i) (in descending order)
6) $|P^{k+1}| = |P^{k+1}| \cup F_i$ (N-$|P^{k+1}|$ (Choose the first N-$|P^{k+1}|$ elements of F_i)
7) Q^{k+1} (use selection, crossover and mutation to create a new population with using P^{k+1}). Set k=k+1.

B. Best Compromise Solution

Once the Pareto optimal set is obtained, it is practical to choose one solution from all solutions that satisfy different goals to some extends. Due to the imprecise nature of the decision maker's (DM) judgment, it is natural to assume that the DM may have fuzzy or imprecise nature goals of each objective function [1]. Hence, the membership functions are introduced to represents the goals of each objective function; each membership function is defined by the experiences and intuitive knowledge of the decision maker.

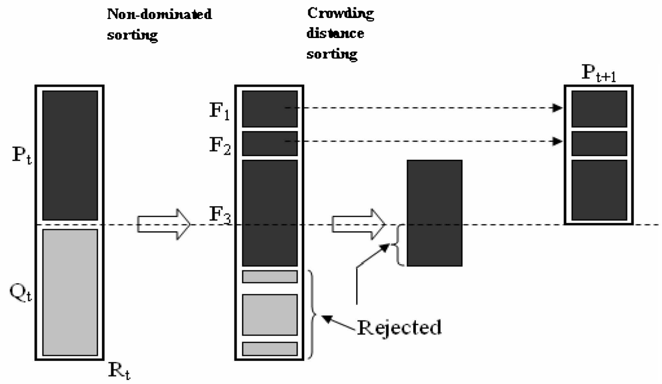

Fig. 2. NSGA-II procedure.

In this study, a simple linear membership function was considered for each of the objective functions. The membership function is defined as follows [15]:

$$\mu_i = \begin{cases} 1 & F_i \le F_i^{\min} \\ \dfrac{F_i^{\max} - F_i}{F_i^{\max} - F_i^{\min}} & F_i^{\max} < F_i < F_i^{\min} \\ 0 & F_i \ge F_i^{\max} \end{cases} \tag{31}$$

Where, F_i^{min} and F_i^{max} are the minimum and the maximum value of the i^{th} objective function among all non-dominated solutions, respectively. The membership function μ_i is varied between 0 and 1, where $\mu_i = 0$ indicates the incompatibility of the solution with the set, while $\mu_i = 1$ means full compatibility.

For each non-dominated solution k, the normalized membership function μ^k is calculated as:

$$\mu^k = \frac{\sum_{i=1}^{N_{obj}} \mu_i^k}{\sum_{k=1}^{M} \sum_{i=1}^{N_{obj}} \mu_i^k} \tag{32}$$

Where M is the number of non-dominated solutions and N_{obj} is the number of objective functions. The function μ_k can be considered as a membership function of non-dominated solutions in a fuzzy set, where the solution having the maximum membership in the fuzzy set is considered as the best compromise solution.

V. Simulation and Discussion

The NSGA-II algorithm has been carried out on the IEEE 30-bus test system [23],[24] and a practical of Java-Bali 24-bus of Indonesian grid system [25]. The generators have been modeled as PV buses with Q limits; the loads are typically represented as constant PQ loads with constant power factor, and increased according to (9) and (10).

The decision variables considered, are the locations and settings of UPFC. The number of UPFC and their constraints are chosen at the beginning; where the number of UPFC is fixed at one. The placement of UPFC is considered as a discreet variable, where all the lines of the system (except line with transformer) are selected to be the optimal location of the UPFC. The parameters of NSGA-II for all optimization cases are summarized in Table I.

TABLE I
NSGA-II Parameters

Population	Generation$_s$	Pool Size	Tour Size	η_c	η_m
100	50	25	2	20	20

From Pareto dominance viewpoint, the extreme points of the Pareto front present the optimal solution of each objective optimized individually. As a matter of fact, in order to evaluate the diversity characteristic of the obtained solutions, the best compromise solution points of Pareto front are compared with the optimal solution of the correspondent objective optimized with the best system loadability (Max. *SL*) and the best active power losses (Min. P_{loss}) by considering the installation cost of UPFC (*IC*) for each of the objectives.

A. IEEE 30- Bus System

The bus data and line data of IEEE 30-bus system are taken from [23],[24] and contain 41 lines. Table III is summarized the extreme points obtained by NSGA-II. Prom Table III it is clear that the installation of UPFC at line 6-8 with the shunt and series setting of 0.94 pu. and -76.73 %, by considering stability constraints, respectively provides the best *SL* of 262.74%. Similarly, by placing the device at the same line, but with the shunt and series settings of 1.02 p.u. and 10.43 %, respectively provides the best P_{loss} of 0.0693 pu.

TABLE III
NSGA-II Solutions of UPFC Placement in IEEE 30-Bus System for Bi-Objective Optimization.

UPFC	Without Stability Constraints			With Stability Constraints		
	Min. P_{loss}	Max. SL	Best Comp Solution	Min. P_{loss}	Max. SL	Best Comp. Solution
Location (lines)	6-4	6-7	6-7	6-8	6-8	6-8
Shunt Setting	1.01	0.94	1.01	1.02	0.94	1.02
Series Setting	6.70	4.29	6.70	10.43	-76.73	5.05
P_{loss} (p.u.)	0.1387	0.4670	0.1387	0.0693	0.3863	0.0821
SL (%.)	188.54	272.95	188.54	157.03	262.74	171.03
IC ($\times 10^6$\$)	17.779	14.772	17.779	15.140	22.732	14.790

Furthermore, from all the non-dominated solutions, the installation of UPFC in the same line as well, with the shunt and series settings of 1.02 pu and 5.05 %, considered as the best compromise solution as depicted from the Pareto front of the optimization in Fig. 3. In addition installation cost of the UPFC calculated in this condition is \$ 14.790 million.

The eigenvalue, *FSVI*, and *LQP* which represented the stability of system at the best compromise solution depicts in Figs. 4 and 5, respectively. It is evident that the installation of UPFC assures grid stability with all the eigenvalues in the left hand side of the S-plane during the best compromise solution. Furthermore, the graph does not include the far end stable eigenvalues (real eigenvalue less than -6) in the chart. The voltage and line stability indices (*FVSI* and *LPQ*) are quite less than 1.00 as given in Fig. 9. These indices are used to maintain grid stability at various levels of system loadability witch ensure that no bus will collapse due to overloading and no line is over loaded under any grid condition.

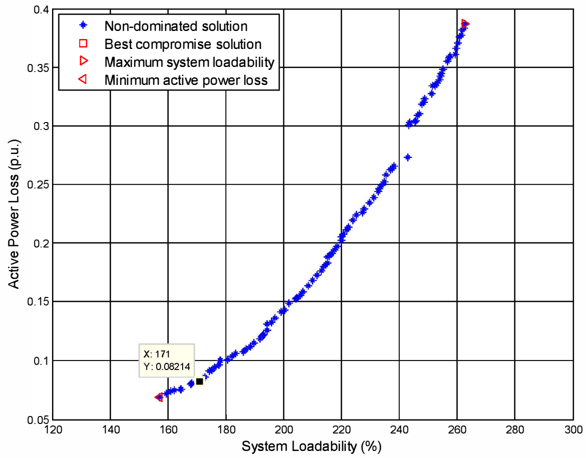

Fig. 3. Pareto front of optimal placement of UPFC for IEEE 30-bus system.

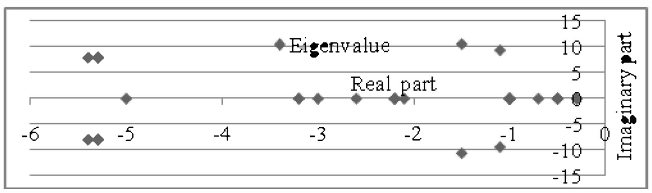

Fig. 4. Eigenvalues of best compromise solution of UPFC placement for IEEE 30-bus system.

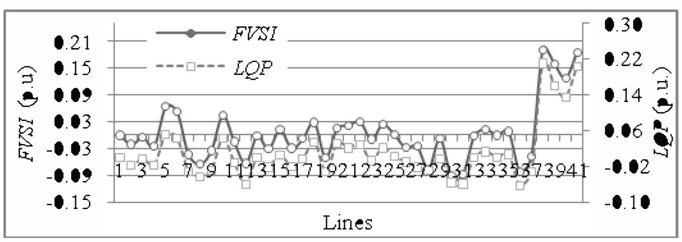

Fig. 5. The best compromise solution of *FVSI* and *LQP* after optimal placement of UPFC in IEEE 30-bus system.

The results obtained from IEEE 30-bus system is compared with the results reported in [5] as shown in Table IV.

TABLE IV
OPTIMAL *IC*, *MSL* AND MINIMUM NUMBER OF UPFC (N) NEEDED IN IEEE 30-BUS SYSTEM.

Type of FACTS	Result obtained in this study				Result reported in [5]			
	SL (%)	N	*IC* ($\times10^6$\$)	Stability Const.	*MSL* (%)	N	*IC* ($\times10^6$\$)	Stability Const.
UPFC	171.03	1	14.790	Yes	139	8	276.7	No

From Table IV it can be seen that, the best compromise solution of *SL* of single UPFC proposed in this study is much higher than the result of maximum system loadability (*MSL*) reported in [5], but the *IC* is quite less than the previous result by installing 8 number of UPFC. Stability constraints and minimization of active power loss are not reported in [5].

B. *Java-Bali 24-Bus Indonesian Grid System*

In order to give a more practical aspect to this study, the proposed method has been applied on the realistic Java-Bali 24-bus Indonesian grid system [25]. Single line diagram of the system is shown at Fig. A.1, the bus data and line data are taken from the Indonesia Government Electrical Company and which has 8 generators and 49 lines. The total active and reactive load of the system is 10570.87 MW and 4549.23 MVAR, respectively.

TABLE V
NSGA-II SOLUTIONS OF UPFC PLACEMENT IN JAVA-BALI 24-BUS INDONESIAN SYSTEM FOR BI-OBJECTIVE OPTIMIZATION

UPFC	Without stability Constraints			With stability Constraints		
	Min. P_{loss}	Max. SL	Best Comp. Solution	Min. P_{loss}	Max. SL	Best Comp. Solution
Location (lines)	19-24	15-21	19-1	19-24	19-1	19-1
Shunt setting	0.99	0.96	0.98	0.99	0.96	0.98
Series setting	18.84	-26.69	20.00	-52.20	18.4	2.04
P_{loss} (p.u.)	2.1222	7.2573	2.3782	1.9562	3.8411	2.3656
SL (%.)	135.86	182.11	153.13	135.83	172.21	154.70
IC ($\times10^6$\$)	54.966	17.674	8.433	48.035	23.178	18.581

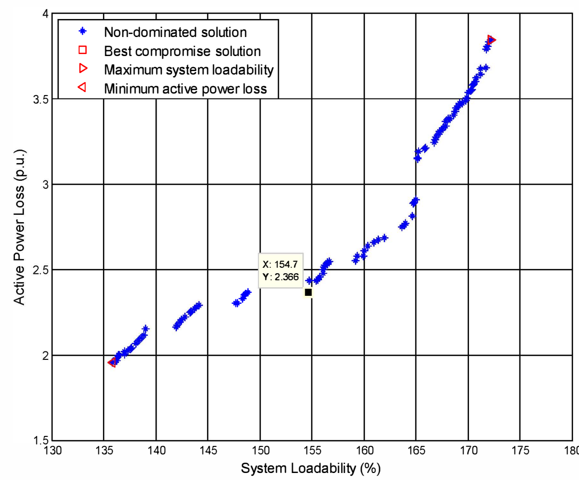

Fig. 6. Pareto front of optimal placement of UPFC for Java-Bali 24-bus.

The results for optimal placement of single UPFC using NSGA-II for Java-Bali 24-bus Indonesian grid system is shown in Table V. The Pareto front of this case is presented in Fig. 6. From Table V, by considering stability constraints, it is observed that the installation of UPFC in line 19-1 with shunt and series settings of 0.96 p.u. and 18.4 %, respectively provides the best *SL* of 172.21%. Also, the installation of a UPFC in line 19-24 with shunt and series settings of 0.99 p.u and -52.20 %, respectively provides the best P_{loss} of 1.9562 pu.

From the decision maker point of view, the best compromise solution in this case is the same location as obtained for the best *SL,* but with shunt and series settings of 0.98 p.u. and 2.04 %, respectively whereas the installation cost of UPFC is \$ 18.581 million. The stability constraints at the best compromise solution that represented by their eigenvalue, *FVSI,* and *LQP* are well within acceptable limits as depicted in Figs. 7 and 8.

From all of these results, it can be concluded that the NSGA-II is able to obtain the optimal location of UPFC devices formulated as multi-objective optimization problem and applied to realistic power system.

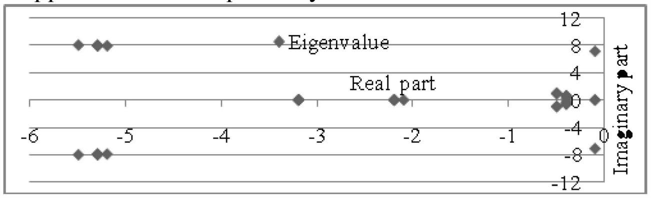

Fig. 7. Eigenvalues of best compromise solution of UPFC placement in Java Bali 24-bus indonesian system.

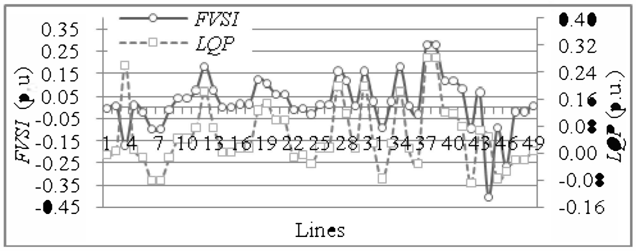

Fig. 8. The best compromise solution of *FVSI* and *LQP* after optimal placement of UPFC in Java-Bali 24-bus Indonesian system.

VI. Conclusion

A potent approach based on NSGA-II algorithm has been presented and applied to optimal location and settings of UPFC in power system. The problem has been formulated as a real mixed continuous integer multi-objective optimization problem, where two different objectives are considered viz., maximization of system loadability and minimization of active power loss in transmission lines whereas maintaining the system security and stability margins, i.e., small signal stability, *FVSI,* and *LQP* in acceptable ranges.

A fuzzy based mechanism has been employed to extract the best compromise solution from the Pareto front. The effectiveness of the proposed method, results obtained for the IEEE 30-bus and a practical Java-Bali 24-bus of Indonesian systems, showed that NSGA-II provides well distributed Non-dominated solutions and well exploration of the research space. Moreover the method does not impose any limitation on the number of objectives and constraints.

VII. Appendix

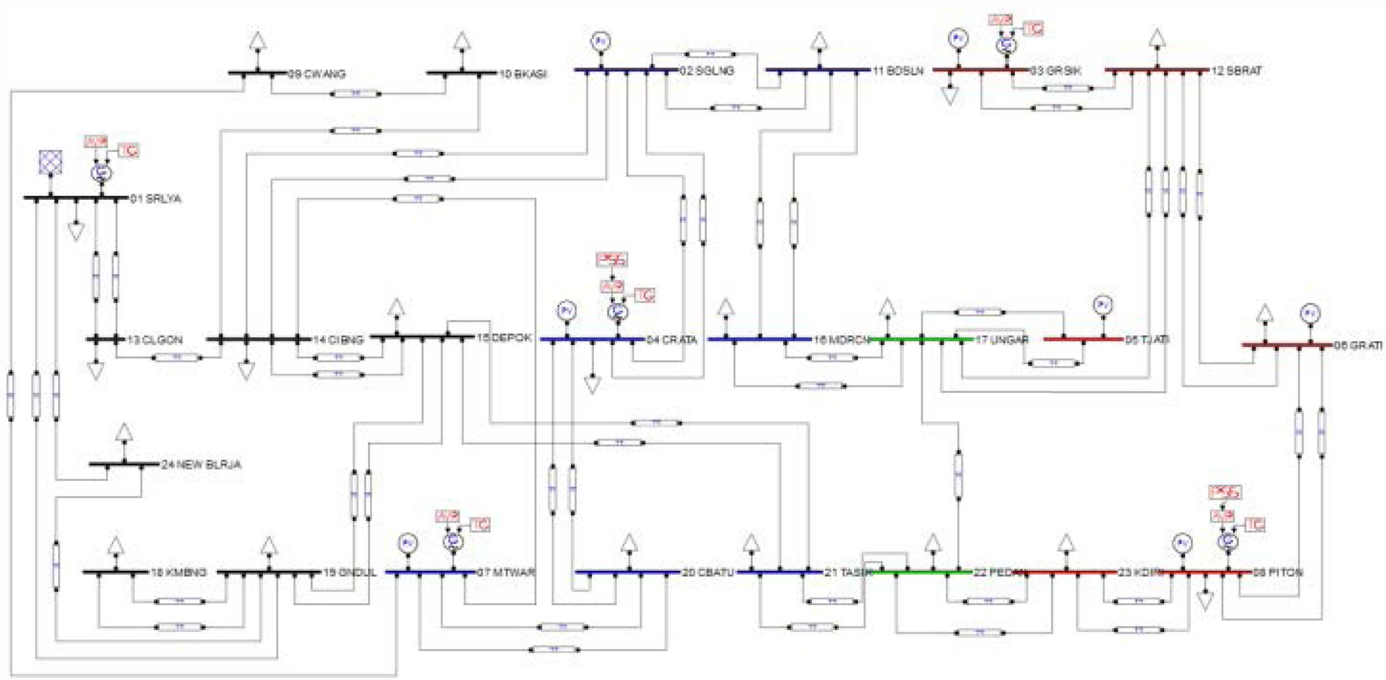

Fig. A.1 Single Line Diagram of Java-Bali 24-Bus Indonesian System.

VIII. Acknowledgment

The authors would like to thank to the Indonesian Government Electrical Company for supporting the data and to Prof. F. Milano for the free PSAT software package.

IX. References

[1] N. G. Hingorani, "Role of FACTS in a deregulated market," in *Power Engineering Society Summer Meeting, 2000. IEEE*, 2000, pp. 1463-1467 vol. 3.

[2] N. G. Hingorani, "Flexible AC transmission," *Spectrum, IEEE,* vol. 30, pp. 40-45, 1993.

[3] D. Povh, "Modeling of FACTS in power system studies," in *Power Engineering Society Winter Meeting, 2000. IEEE*, 2000, pp. 1435-1439 vol.2.

[4] N. Hingorani and L. Gyugyi, *Concepts and Technology of Flexible AC Transmission Systems*, 1999.

[5] M. Saravanan, *et al.*, "Application of particle swarm optimization technique for optimal location of FACTS devices considering cost of installation and system loadability," *Electric Power Systems Research,* vol. 77, pp. 276-283, 2007.

[6] J. G. Singh, *et al.*, "Placement of FACTS controllers for enhancing power system loadability," in *Power India Conference, 2006 IEEE*, 2006, p. 7 pp.

[7] P. Bhasaputra and W. Ongsakul, "Optimal placement of multi-type FACTS devices by hybrid TS/SA approach," in *Circuits and Systems, 2003. ISCAS '03. Proceedings of the 2003 International Symposium on*, 2003, pp. III-375-III-378 vol.3.

[8] P. Jirapong and W. Ongsakul, "Optimal placement of multi-type FACTS devices for total transfer capability enhancement using hybrid evolutionary algorithm," *Electric Power Components and Systems,* vol. 35, pp. 981-1005, 2007.

[9] S. Gerbex, *et al.*, "Optimal location of multi-type FACTS devices in a power system by means of genetic algorithms," *Power Systems, IEEE Transactions on,* vol. 16, pp. 537-544, 2001.

[10] L. J. Cai, *et al.*, "Optimal choice and allocation of FACTS devices in deregulated electricity market using genetic algorithms," in *Power Systems Conference and Exposition, 2004. IEEE PES*, 2004, pp. 201-207 vol.1.

[11] Z. Lu, *et al.*, "Optimal allocation of FACTS devices with multiple objectives achieved by bacterial swarming algorithm," in *Power and Energy Society General Meeting - Conversion and Delivery of Electrical Energy in the 21st Century, 2008 IEEE*, 2008, pp. 1-7.

[12] S. Nagalakshmi and N. Kamaraj, "Loadability enhancement for pool model with FACTS devices in transmission system using Differential Evolution and Particle Swarm Optimization," in *Power Electronics (IICPE), 2010 India International Conference on*, 2011, pp. 1-8.

[13] H. I. Shaheen, *et al.*, "Application of Evolutionary Optimization Techniques for Optimal Location and Parameters Setting of Multiple UPFC Devices," in *Natural Computation, 2007. ICNC 2007. Third International Conference on*, 2007, pp. 688-697.

[14] G. I. Rashed, *et al.*, "Optimal Location and Parameter Settings of Multiple TCSCs for Increasing Power System Loadability Based on GA and PSO Techniques," in *Natural Computation, 2007. ICNC 2007. Third International Conference on*, 2007, pp. 335-344.

[15] R. Benabid, *et al.*, "Optimization of UPFCs using hierarchical multi-objective optimization algorithms," *Analog Integrated Circuits and Signal Processing,* pp. 1-12, 2011.

[16] F. Milano, "An Open Source Power System Analysis Toolbox," *Power Systems, IEEE Transactions on,* vol. 20, pp. 1199-1206, 2005.

[17] P. Kumkratug and M. H. Haque, "Versatile model of a unified power flow controller in a simple power system," *Generation, Transmission and Distribution, IEE Proceedings-,* vol. 150, pp. 155-161, 2003.

[18] R. Benabid, *et al.*, "Optimal location and setting of SVC and TCSC devices using non-dominated sorting particle swarm optimization," *Electric Power Systems Research,* vol. 79, pp. 1668-1677, 2009.

[19] I. Musirin and T. K. Abdul Rahman, "Novel fast voltage stability index (FVSI) for voltage stability analysis in power transmission system," in *Research and Development, 2002. SCOReD 2002. Student Conference on*, 2002, pp. 265-268.

[20] M. V. Suganyadevia and C. K. Babulal, "Estimating of loadability margin of a power system by comparing Voltage Stability Indices," in *Control, Automation, Communication and Energy Conservation, 2009. INCACEC 2009. 2009 International Conference on*, 2009, pp. 1-4.

[21] K. Deb, *et al.*, "A fast and elitist multiobjective genetic algorithm: NSGA-II," *Evolutionary Computation, IEEE Transactions on,* vol. 6, pp. 182-197, 2002.

[22] L. Yang, "A fast and elitist multi-objective particle swarm algorithm: NSPSO," in *Granular Computing, 2008. GrC 2008. IEEE International Conference on*, 2008, pp. 470-475.

[23] R. D. Zimmerman, *et al.*, "MATPOWER: Steady-State Operations, Planning, and Analysis Tools for Power Systems Research and Education," *Power Systems, IEEE Transactions on,* vol. 26, pp. 12-19, 2011.

[24] O. Alsac and B. Stott, "Optimal Load Flow with Steady-State Security," *Power Apparatus and Systems, IEEE Transactions on,* vol. PAS-93, pp. 745-751, 1974.

[25] P3B, "The 2010 Operation Plan," The Indonesian Government Electrical Company, *PT PLN (PERSERO)*, Cinere 61514, Jakarta Selatan, Indonesia, 2010.

X. Biographies

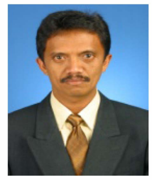

I Made Wartana received his B. Eng. and M. Eng. from Electrical Engineering Department, National Institute of Technology (ITN) Malang, East of Java, Indonesia and Bandung Institute of Technology (ITB), Indonesia in 1986 and 1994 respectively. He has been an Assistant Professor at National Institute of Technology (ITN) Malang, Indonesia since 1994.

He is currently pursuing his doctoral degree from Asian Institute of Technology, Thailand. His research interests are in application of FACTS devices in power grid, AI application to power system, and in grid integration of renewable.

Jai Govind Singh received his M. Tech. and Ph.D. degrees in Electrical Engineering from I.I.T. Rookree, and IIT Kanpur India, in 2003 and 2008, respectively. He is currently Assistant Professor in the energy field of study, Asian Institute of Technology, Thailand. His research interests include power system operation and control, FACTS, power sector deregulation and power system planning.

Weerakorn Ongsakul received the M.S. and Ph.D. degrees in electrical engineering from Texas A&M University, College Station, USA in 1991 and 1994, respectively. He is currently Associate Professor and Dean of School of Environment, Resources and Development, Asian Institute of Technology, Thailand. His current interests are in parallel processing applications, AI applications to power systems, and power system restructuring and deregulation.

Kittavit Buayai (M'08) received B. Eng from Rajamangala Institute of Technology and M. Eng. from Khon Kean University, Thailand, all degrees in electrical engineering, in 1993 and 1997 respectively.He has been an Assistant Professor at Rajamangala University of Technology Isan, Nakhonratchasima, Thailand since 2002. He is currently working toward the D.Eng. at the Asian Institute of Technology, Pathumthani, Thailand. Current research interests are in the field of Micro Grid in distribution network planning optimization, power quality, and an application of geographic information system in power system.

Sasidharan Sreedharan was born in Kerala, India in 1974. He received his B.Tech and M.Tech degree in Electrical Power System from Govt Engineering College, Thrissur, Kerala, India in 1995 and 1997 respectively. In 2010 he received his D.Eng at Asian Institute of Technology, Thailand. His research interests are in grid integration of renewable, AI applications to power systems and grid stability.